Similarity Solution of Axisymmetric Stagnation-Point Flow and Heat Transfer of a Nanofluid on a Stationary Cylinder with Constant Wall Temperature

Hamid Mohammadiun, Vahid Amerian, Mohammad Mohammadiun & Asghar B. Rahimi

Iranian Journal of Science and Technology, Transactions of Mechanical Engineering

ISSN 2228-6187
Volume 41
Number 1

Iran J Sci Technol Trans Mech Eng
(2017) 41:91-95
DOI 10.1007/s40997-016-0022-8

Iran J Sci Technol Trans Mech Eng (2017) 41:91–95
DOI 10.1007/s40997-016-0022-8

TECHNICAL NOTE

Similarity Solution of Axisymmetric Stagnation-Point Flow and Heat Transfer of a Nanofluid on a Stationary Cylinder with Constant Wall Temperature

Hamid Mohammadiun[1] · Vahid Amerian[2] · Mohammad Mohammadiun[1] · Asghar B. Rahimi[3]

Received: 22 May 2015 / Accepted: 12 January 2016 / Published online: 1 November 2016

Abstract The steady state, viscous flow and heat transfer of a nanofluid in the vicinity of an axisymmetric stagnation point of a stationary cylinder is investigated. Exact solution of the Navier–Stokes equations and energy equation are derived in this problem. For all Reynolds numbers, as the particle fraction increases, the depth of diffusion of the thermal boundary layer and shear stresses decreases. It's clear that by adding nanoparticles to the base fluid there is a significant enhancement in convective heat transfer coefficient and convective heat flux.

Keywords Nanofluid · Stagnation-point flow · Convective heat transfer coefficient · Stationary cylinder · Self-similar solution

✉ Hamid Mohammadiun
hmohammadiun@iau-shahrood.ac.ir

Vahid Amerian
vahid.mech86@gmail.com

Mohammad Mohammadiun
mmohammadiun@iau-shahrood.ac.ir

Asghar B. Rahimi
rahimiab@um.ac.ir

1 Department of Mechanical Engineering, Shahrood Branch, Islamic Azad University, Shahrood, Iran

2 Department of Mechanical Engineering, Shahrood University, Shahrood, Iran

3 Faculty of Engineering, Ferdowsi University of Mashhad, Mashhad, Iran

1 Introduction

Convective heat transfer is very important for many industrial heating or cooling equipment. An innovative way of improving the thermal conductivities of fluids is to suspend small solid particles in the fluid. Maxwell (1881) showed the possibility of increasing thermal conductivity of a mixture by more volume fraction of solid particles called nanofluid. In recent years, many researches have been performed to study the effects of nanofluid on convective heat transfer rate.

Wang (1974) was first to find exact solution for the problem of axisymmetric stagnation flow on an infinite stationary circular cylinder. In another investigation, Saleh and Rahimi (2004) presented the results of a stagnation flow on a moving cylinder with transpiration where Reynolds number was considered for high values. In a study performed by Tahavvor (2013), experimental and numerical results of a turbulent axisymmetric impinging jet flow were presented. He considered the flow on a circular cylinder with both offset and non-offset situations. Gorla (1978a, b, 1979), in a series of papers, studied the steady and unsteady flows over a circular cylinder in the vicinity of the stagnation point for the cases of constant axial movement and the special case of axial harmonic motion of a non-rotating cylinder. Recently, Mohammadiun and Rahimi (2012) have investigated the stagnation-point flow and heat transfer of a viscous, compressible fluid on a cylinder.

In the present analysis, for the first time the heat transfer enhancement of steady viscous flow of nanofluid in the vicinity of an axisymmetric stagnation point of a stationary cylinder is considered. It is interesting to note that in current work the thermal conductivity coefficient of nanofluid is considered temperature-dependent and the ordinary differential equation has been derived. An exact solution of the Navier–Stokes equations is obtained. The self-similar solution is reached by introducing the similarity variables. Sample distributions of shear stress, temperature and the convective heat transfer coefficient at Reynolds numbers ranging from 0.1 to 1000 are presented for different values of particle volume fractions.

2 Properties of Nanofluid

The aluminum oxide (γAl_2O_3) nanoparticles which have been used in this research have the following characteristics (Table 1).

3 Problem Formulation

Flow is considered in cylindrical coordinates (r, z) with corresponding velocity components (u, w). A reduction of the Navier–Stokes equations (Tahavvor 2013; Gorla 1978a, b; 1979) is obtained by the following coordinate separation of the velocity field which is actually modeled by the form of their limits, and introducing $\eta\left(\frac{r}{a}\right)^2-1$, we have:

$$u = -\bar{k}\frac{a}{\sqrt{\eta+1}}f(\eta), \quad w = 2\bar{k}f'(\eta)z, \quad p = \rho_n \bar{k}^2 a^2 P \tag{1}$$

Note that, for the case of base fluid ($\phi_\upsilon = 0$), this variable is similar to the one in Wang (1974), except that it changes from zero to infinity instead of one to infinity. Transformations (1) yields an ordinary differential equation in terms of $f(\eta)$

$$(\eta+1)f''' + f'' + Re_n\left[1-(f')^2+ff''\right] = 0 \tag{2}$$

In these equations,

$$Re = \frac{\bar{k}a^2}{2\nu_f} \tag{3}$$

$$Re_n = \beta Re \tag{4}$$

$$\beta = \left[1-34.87\left(\frac{d_p}{d_f}\right)^{-0.3}\phi_v^{1.03}\right]\left(1-\phi_v+\phi_v\frac{\rho_p}{\rho_f}\right) \tag{5}$$

To transform the energy equation into a non-dimensional form, we introduce $\theta(\eta) = \frac{T(\eta)-T_\infty}{T_w-T_\infty}$, therefore, by using Corcione's correlation and introducing Γ as

$$\Gamma = 4.4\left(\frac{2\rho_{\mathrm{bf}}k_b}{\pi\mu_{\mathrm{bf}}^2 d_p}\right)^{0.4}\frac{1}{T_{fr}^{10}}\left(\frac{k_p}{k_f}\right)^{0.03} \tag{6}$$

The energy equation can be written as

$$\begin{aligned}&\left\{1+\Gamma\phi_v^{0.66}\mathrm{Pr}_{bf}^{0.66}[T_\infty+(T_w-T_\infty)\theta]^{10.4}\right\}[(\eta+1)\theta''+\theta'] \\ &\quad + 10.4[T_\infty+(T_w-T_\infty)\theta]^{9.4}(T_w-T_\infty)\Gamma\phi_v^{0.66}\mathrm{Pr}_{\mathrm{bf}}^{0.66}(\eta+1)(\theta')^2 \\ &\quad + \left\{1-\phi_v+\phi_v\left[\frac{(\rho c_p)_p}{(\rho c_p)_f}\right]\right\}Re_{bf}\mathrm{Pr}_{bf}f\theta' = 0\end{aligned} \tag{7}$$

Boundary conditions are as follows:

$$\begin{aligned}&\eta = 0: f = 0, \quad f' = 0 \quad \theta = 1 \\ &\eta \to \infty: f' = 1 \quad \theta = 0\end{aligned} \tag{8}$$

The convective heat transfer coefficient is obtained from:

$$\begin{aligned}h &= -2k_{\mathrm{nf}}|_{T=T_w}\theta'(0) \\ &= -2k_{\mathrm{bf}}\left[1+4.4Re_p^{0.4}\mathrm{Pr}_{\mathrm{bf}}^{0.66}\left(\frac{T_w}{T_{fr}}\right)^{10}\left(\frac{k_p}{k_f}\right)^{0.03}\phi_v^{0.66}\right]\theta'(0)\end{aligned} \tag{9}$$

The shear stress on the surface of the cylinder is obtained from:

$$\sigma = \mu_n[2\bar{k}f''(0)z]\frac{2}{a} \Rightarrow \frac{\sigma a}{4\mu_n\bar{k}z} = f''(0) \tag{10}$$

Equations (2) and (7) along with boundary conditions (8) have been solved by using the fourth-order Runge–Kutta method of integration along with a shooting method, Press et al. (1997).

Table 1 Characteristics and correlation used in current study

Property	Relation
Density	$\rho_n = (1-\phi_v)\rho_f + \rho_p$
Viscosity (Corcione 2011)	$\frac{\mu_n}{\mu} = \frac{1}{1-34.87\left(\frac{d_p}{d_f}\right)^{-.03}\phi_v^{1.03}}$, where $d_f = 0.1\left(\frac{6M}{N\pi\rho_{f0}}\right)^{\frac{1}{3}}$
Thermal conductivity (Corcione 2011)	$\frac{k_{eff}}{k_f} = 1+4.4Re_p^{0.4}\mathrm{Pr}_{\mathrm{bf}}^{0.66}\left(\frac{T}{T_{\mathrm{fr}}}\right)^{10}\left(\frac{k_p}{k_f}\right)^{0.03}\phi_v^{0.66}$ where $\mathrm{Re}_p = \frac{2\rho_{\mathrm{bf}}k_bT}{\pi\mu_{\mathrm{bf}}^2 d_{\mathrm{p}}}$ and $\mathrm{Pr}_{\mathrm{bf}} = \frac{\mu_{\mathrm{bf}}(c_p)_{\mathrm{bf}}}{k_{\mathrm{bf}}}$

4 Results and Discussion

In this section, the solution of the self-similar Eqs. (2) and (7), along with surface shear stresses and convective heat transfer coefficient for prescribed values of surface temperature for selected values of Reynolds numbers and particle volume fraction is presented.

Sample profiles of the $\theta(\eta)$ function against η for the case of constant surface temperature for $\phi_\upsilon = 0.02, T_w = 450$ K, and for selected values of Reynolds numbers are depicted in Fig. 1. As expected, the momentum is increased with the Reynolds number and consequently, the thermal layer thickness is decreased once the thermal diffusion is overcome, as can be observed in the following figures.

Effect of variations of particle fraction factor on $\theta(\eta)$ function against η for $T_w = 450$ K and selected value of Reynolds number is presented in Fig. 2. For $\phi_\upsilon = 0$ base fluid, the result of Gorla (1976) is extracted; it is interesting to note that, as ϕ_υ increases, the absolute value of the dimensionless temperature gradient is decreased at surfaces; nevertheless, this decreasing rate is negligible compared to that of increasing rate in the thermal conductivity. Therefore, the heat transfer coefficient is increased through addition of nanoparticles.

Sample profiles of the convective heat transfer coefficient h against Reynolds number for $\phi_\upsilon = 0.02$ and $\phi_\upsilon = 0.05$ and for selected values of wall temperature are depicted in Fig. 3. When the wall temperature or Reynolds number increases, the thermal boundary layer thickness increases. Moreover, in the interaction between the decreasing rate of dimensionless temperature gradient and increasing rate of thermal conductivity coefficient, a more significant effect is reported for the heat transfer coefficient.

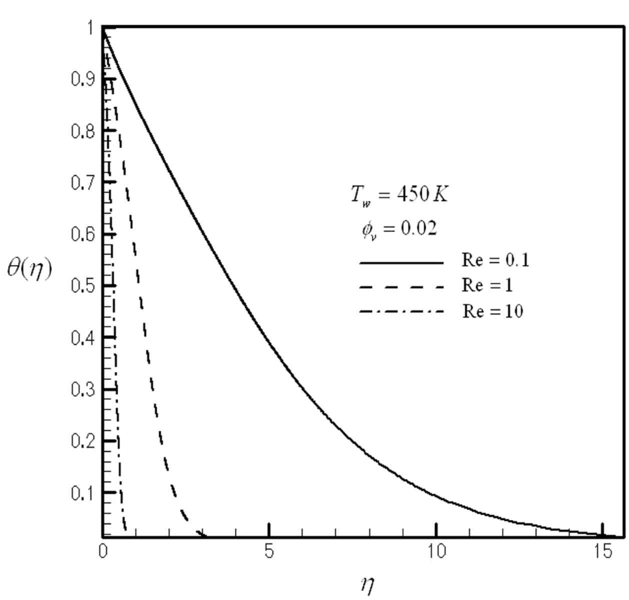

Fig. 1 Variation of θ in terms of η at $T_w = 450$ K and $\phi_v = 0.02$ for different values of Reynolds number

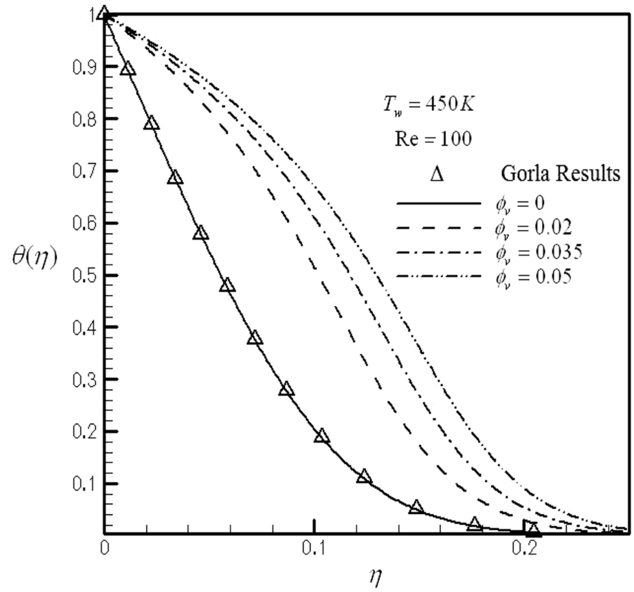

Fig. 2 Variation of θ in terms of η at $T_w = 450$ K and Re = 100 for different values of particle fractions

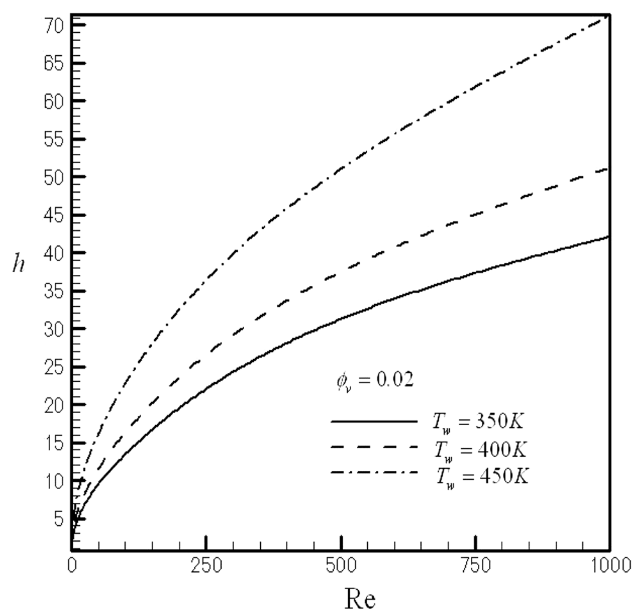

Fig. 3 Variation of h in terms of Re at $\phi_\upsilon = 0.02$ for different values of wall temperature

Effect of variations of particle fraction factor on h against Re for selected value of T_w is presented in Fig. 4. It is interesting to note that, as ϕ_υ increases, the depth of the diffusion of the thermal boundary layer increases. Based on the figures, an increase in the wall temperature and the Reynolds number along with addition of nanoparticles will result in increased heat transfer coefficient.

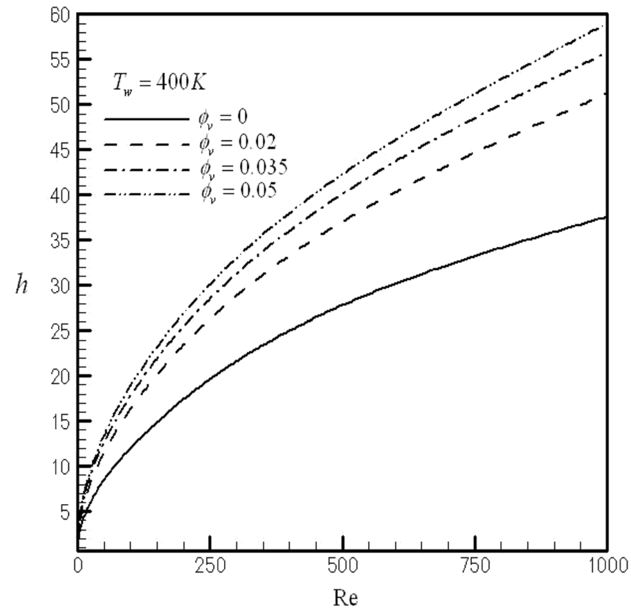

Fig. 4 Variation of h in terms of Re at $T_w = 400$ K for different values of particle fractions

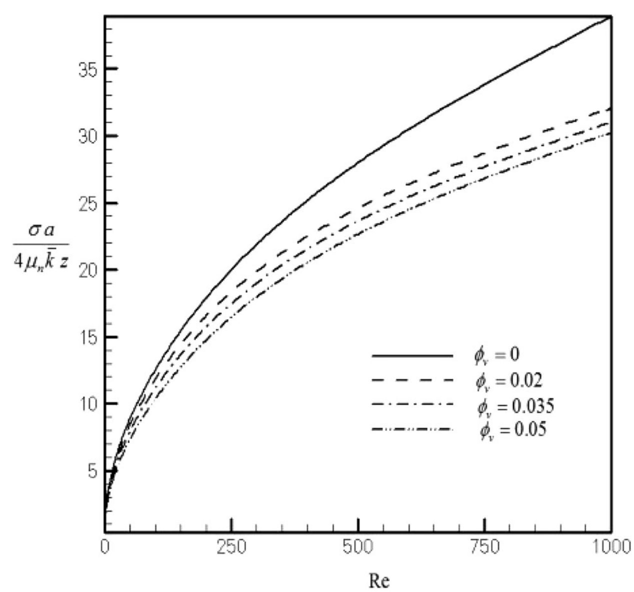

Fig. 5 Variation of shear stress in terms of Re and for different values of particle volume fraction

Sample profiles of surface shear stress against Reynolds Number are shown in Fig. 5, for selected values of particle volume fraction. As expected, as the particle volume fraction increases because of decreasing in the velocity gradient on the cylinder wall, the surface shear stress decreases.

Sample profiles of surface shear stress against particle volume fraction are shown in Fig. 6, for selected values of Reynolds numbers. As expected, by increasing the

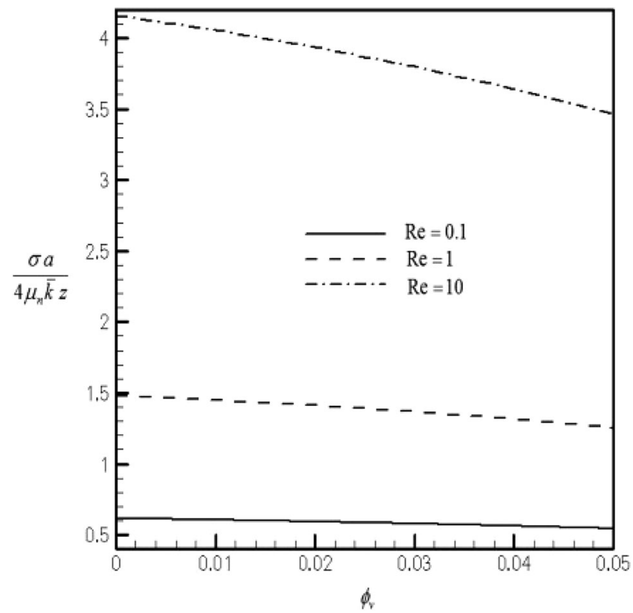

Fig. 6 Variation of shear stress in terms of ϕ_υ and for different values of Reynolds number

Reynolds number the momentum boundary layer thickness decreases and the velocity gradient on the surface increases. Increasing of the velocity gradient on the surface leads to increase in the surface shear stress.

5 Conclusions

An exact solution for the Navier–Stokes equations and energy equation has been obtained for the problem of axisymmetric stagnation-point flow of a nanofluid on a stationary cylinder. A reduction of these equations is obtained by the use of appropriate transformations introduced for the first time. The general self-similar solution is obtained when the wall temperature of the cylinder is constant. It can be said that for all Reynolds numbers and cylinder wall temperatures, as ϕ_υ increases the shear stresses decreases and heat transfer coefficient increases. It is proposed to consider different movements of the cylinder; for instance, an oscillating cylinder might be applicable. Further, applying Rheology approach can be considered as another future opportunity.

References

Corcione M (2011) Empirical-correlating equations for predicting the effective thermal conductivity and dynamic viscosity of nanofluids. Energy Convers Manag 52:789–793

Gorla RSR (1976) Heat transfer in an axisymmetric stagnation flow on a cylinder. Appl Sci Res 32:541–553

Gorla RSR (1978a) Nonsimilar axisymmetric stagnation flow on a moving cylinder. Int J Eng Sci 16:397–400

Gorla RSR (1978b) Transient response behavior of an axisymmetric stagnation flow on a circular cylinder due to time dependent free stream velocity. Int J Eng Sci 16:493–502

Gorla RSR (1979) Unsteady viscous flow in the vicinity of an axisymmetric stagnation-point on a cylinder. Int J Eng Sci 17:87–93

Maxwell JC (1881) A treatise on electricity and magnetism. Oxford Univ. Press, Cambridge

Mohammadiun H, Rahimi AB (2012) Stagnation-point flow and heat transfer of a viscous, compressible fluid on a cylinder. J Thermophys Heat Trans 26:494–502

Press WH, Flannery BP, Teukolsky SA, Vetterling WT (1997) Numerical recipes: the art of scientific computing. Cambridge University Press, New York **548**

Saleh R, Rahimi AB (2004) Stagnation flow and heat transfer on a moving cylinder with transpiration and high Reynolds number consideration. Iran J Sci Technol Trans Mech Eng 28(4):453–466

Tahavvor AR (2013) Experimental and numerical study of a turbulent axisymmetric jet impinging onto a circular cylinder in offset and non-offset situations. Iran J Sci Technol Trans Mech Eng 37:63–70

Wang C (1974) Axisymmetric stagnation flow on a cylinder. Q Appl Math 32:207–213